Evolutionary models of color categorization. I. Population categorization systems based on normal and dichromat observers

Kimberly A. Jameson[1,3] and Natalia L. Komarova[2,4]

[1]*Institute for Mathematical Behavioral Sciences, University of California, Irvine, Social Science Plaza, Irvine, California 92697-5100, USA*
[2]*Department of Mathematics, University of California, Irvine, Rowland Hall, Irvine, California 92697-3975, USA*
[3]*kjameson@uci.edu*
[4]*komarova@math.uci.edu*

The evolution of color categorization is investigated using artificial agent population categorization games, by modeling observer types using Farnsworth–Munsell 100 Hue Test performance to capture human processing constraints on color categorization. Homogeneous populations of both normal and dichromat agents are separately examined. Both types of populations produce near-optimal categorization solutions. While normal observers produce categorization solutions that show rotational invariance, dichromats' solutions show symmetry-breaking features. In particular, it is found that dichromats' local confusion regions tend to repel color category boundaries and that global confusion pairs attract category boundaries. The trade-off between these two mechanisms gives rise to population categorization solutions where color boundaries are anchored to a subset of locations in the stimulus space. A companion paper extends these studies to more realistic, heterogeneous agent populations [J. Opt. Soc. Am. A **26**, 1424–1436 (2009)]. © 2009 Optical Society of America

OCIS codes: 330.1690, 330.5020, 330.4060.

1. INTRODUCTION

The empirical literature on human color perception and categorization suggests that there is a good deal of universality in color categorization across different groups of people, although a considerable amount of variation is observed across individual categorizers and ethnolinguistic categorization systems [1]. A long-standing debate in the field is whether specific universal tendencies exist in the ways different human linguistic societies categorize and name perceptual color experiences and if so, what factors (e.g., physical environment, human biology, perception, social features) cause them. A major challenge for the area continues to be development of a theory that accounts for universal patterns seen across various color categorization systems while simultaneously explaining observed differences. This color categorization, color vision, and perceptual processing problem has recently attracted the interest of computational scientists [2–8].

A related issue is whether any consequences for human population categorization systems follow from individual observer color perception differences, which vary by degree and frequency, across populations. It is possible that even considerable amounts of within-population individual variation do not substantially affect categorization solutions across different populations. Alternatively, differences in individual color perception across two populations might very easily produce substantive differences in the categorization systems that the populations evolve and end up using to classify color in everyday discourse.

While a large amount of empirical research compares population categorization data across different language groups (e.g., [9]), very little systematic investigation has focused on the impact of individual differences within populations on those populations' color categorization systems ([10–12] consider some influences of individual differences). In particular, population variation scenarios and their outcomes have not been systematically investigated in light of either (i) empirically observed variation within and across human groups, or (ii) simulations that vary agent-based models of categorization. For the methodology of population categorization simulations, real possibilities exist for investigating many features having counterparts in human color category evolution. For example, it provides a means to observe, *in silico*, the evolutionary dynamics of developing categorization systems, to study system robustness and factors influencing system stabilization, and to evaluate structural similarity or variation in stable solutions that occur under different constraints.

The present paper explores the impact of varying individual visual processing constraints on the evolution of shared color category systems. One goal is to systematically examine the ways color category solutions change as a function of varying perceptual processing features of observer populations. In particular, we focus on the influences from forms of color discrimination deficiencies found in real observers. Another goal is to identify mechanisms contributing to color category development and category solution variation.

The modeling framework used here employs agent-based evolutionary game theory methods to model human color categorization systems [6,8]. While our earlier re-

search considered idealized populations of agents with different color perception abilities, in the present paper we investigate the effect of more realistic observer variation. We aim to gain understanding of the variation in color categorization systems found across homogeneous populations (i.e., populations of simulated observers, or "agents," that all possess the same discrimination model) under different realistic observer models. This contrasts with our companion paper, which examines color categorization for heterogeneous populations ([13] this issue). In the present paper we examine two types of observer variations: (1) normal color perception variations and (2) protanope and deuteranope dichromat variations.

We begin below by describing the stimulus continuum on which all our agent models are based, and detail the agent models used. Then we report investigations that use realistic models of several individual observer types, incorporated into homogeneous population simulations, and present the results. The last section of the article summarizes the findings of the research.

2. MODELING ARTIFICIAL OBSERVER POPULATIONS

Evolutionary game theory methods are used to examine the effects of specific realistic constraints on color categorization and inter-individual communication. These follow a modeling framework in which individual agents learn to (1) categorize simulated colors through reinforcement learning by playing "discrimination–similarity games" and (2) communicate the meaning of categories to each other [6,8]. Three main components of this evolutionary approach are (A) the stimulus space, (B) the observer model, and (C) the evolutionary game. Component (C) is detailed in recent research [6,8]. Components (A) and (B) are described below.

A. The Farnsworth–Munsell 100 Hue Test as a Stimulus Space

Similar to earlier research [6,8], a hue circle is used as a natural perceptual subspace of the color appearance solid. The hue circle has the following characteristics: it is (i) a justified subspace according to models of human color perception [[14], p. 184], (ii) it has value as a structure for distinguishing normal observers from color-deficient observers based on hue circle similarity relations (e.g., [15]), (iii) as a color perception subspace it preserves similarity relations among hue categories regardless of variation in salient hue points across normal individuals, and (iv) use of the hue circle capitalizes on a wealth of existing human color perception data for the purpose of modeling artificial agent observer groups. The hue circle stimulus model employed in the present investigations is the Farnsworth–Munsell 100 hue test, abbreviated FM100 [16].

The FM100 stimulus is a continuous hue circle series, discretized into 85 color "caps" forming a smooth gradient of hue, ostensibly at a fixed level of brightness and a fixed level of saturation [17]. Figure 1 shows an approximation of the 85-cap hue gradient. Our use of the FM100's 85 stimuli as a hue circle continuum extends the comparatively restricted hue continua investigated in our earlier color category studies and permits more direct generalizations and comparisons with available human color perception data (i.e., [18,19]).

B. Realistic Models of Observer Variation

In this paper we model *normal* and *dichromat* agents, and only a subspace of full color space is considered. Therefore, our observer models reflect only the appropriate subset of human color discrimination behaviors. Nevertheless, their investigation is very informative.

Models used to define our agents consider only color perception deficiencies linked to human X-chromosome
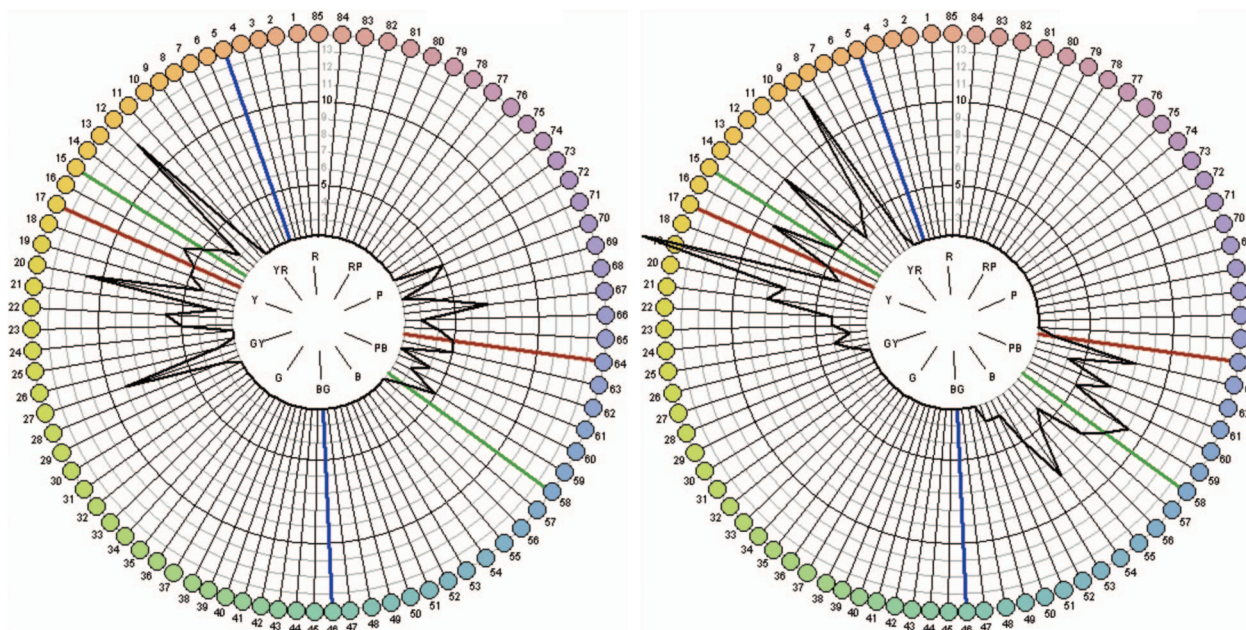

Fig. 1.   FM100 stimulus with data used to model protanope (left) and deuteranope (right) agents. Colored lines show deficiency confusion axes: red=protan, green=deutan. (Blue=tritan; not modeled here). Deviations from the inner circle illustrate observer sorting errors.

recessive inheritance (i.e., protan and deutan variations). The biological bases and perceptual consequences of these forms of human deficiency are well understood [20]. In protan defects the long-wavelength-sensitive photopigment is missing or abnormal. In deutan defects the middle-wavelength-sensitive photopigment is missing or abnormal. Protan and deutan degrees of color confusion can be summarized as confusions among colors within the sets of (1) green-yellows, yellows, and yellow-reds; (2) browns and greens; (3) blue-greens and violets; and (4) purples, grays, and greens [20]. Such deficiencies occur, for example, among males of European descent at about 8% frequency [20], but incidence of deficiency varies across populations of different ancestry and follow known inheritance patterns [21–24].

Important features distinguish color perception and categorization dynamics in human populations from the scenarios simulated here. Here we minimize learned cognitive factors that contribute to human color categorization—e.g., factors involving individual color memory, social utility attached to specific colors, or personal color salience. Omitting complex cognitive factors here permits a focus on specifically clarifying the influences of color perception and discrimination on categorization. In addition, unlike our recent investigations [6,8], the present study does not examine differing saliences in color space that are linked to either variation in environmental color distribution, or variation in the putative importance or utility, of color (cf. [11]).

C. Modeling Different Forms of Observer Variation

We simulate both normal and deficient observer groups using human data. "Normal" agents include those modeled on normal trichromat FM100 performance data, with trichromacy confirmed by pseudoisochromatic plate assessment [25]. "Deficient" agents are modeled using protanope and deuteranope performances from an FM100 diagnostic database [26].

To accurately model data from normal and deficient human individuals, a probabilistic observer model is introduced. Suppose the hue circle to be categorized by all agents is identical (i.e., the FM100 stimulus). Two colors are chosen randomly from the circle and presented to the agent. The agent must judge whether the two colors are the same or different. An appropriate color confusion transformation can be defined to give the probabilities that an agent perceives the two chosen color stimuli as the same or different in color. In general the transformation is described as a stochastic $n \times n$ matrix (a matrix whose rows sum up to one), $\{C_{ij}\}$, whose entries C_{ij} give the probability that stimulus i is perceived as stimulus j. This confusion matrix varies across individual agents.

In modeling our agents, several types of discrimination-based confusions among FM100 stimuli are defined. One is a form of unsystematic noise in an agent's categorization that resembles the sorting confusion errors seen when human observers sort the FM100 stimulus continuum. Two additional kinds of confusions— referred to as local and global confusions—are also modeled. All forms of confusions are defined below.

1. Sorting Confusions

A human observer may have perfectly normal color perception and be expected to show error-free FM100 sorting performance; however, typically, individual sorting performance shows random transposition errors, or confusions, that occur between adjacent stimuli. Normal confusions tend to be 2-cap exchange errors that are random, seldom reoccur on retest, and are not bunched in any one region of the hue circle [27]. Such normal, unbiased sorting confusions are modeled here by assuming that with probability p, each color cap can be confused with either of its neighboring caps on the FM100 stimulus. This leads to the following matrix:

$$C_{ij}^{sorting} = \begin{cases} 1-p, & i=j \\ p/2, & j=i \pm 1 \\ 0, & \text{otherwise} \end{cases}. \tag{1}$$

FM100 sorting confusion errors [Eq. (1)] are the only confusions modeled and varied in our normal trichromat agents. (Other trichromats, e.g., anomalous trichromats, require additional modeling features to approximate their FM100 performance [13]). Dichromat agent models used here require the parameterization of two additional forms of FM100 confusion, described below.

2. Local Confusions

Local confusions are cap transpositions beyond sorting confusions. They define sizable segments of neighboring FM100 stimuli (mostly within, but also spanning, FM100 trays). *Local confusions* for deficient observers cluster inside *local confusion* regions, or portions of the FM100 continuum where several adjacent stimuli may be confused with one another (see [20,27]), where dichromats may transpose the stimulus order by as much as ten steps or more on the circle. While transpositions in the sequential stimulus order can appear anywhere in an FM100 tray, if local mis-sorting occurs at the end of a given tray there is a tendency for transpositions to continue in the FM100 tray adjacent to the mis-sorted segment. Thus, local confusion regions, as defined here, can span two trays of the FM100, and where they occur typically depends on the severity and type of observer deficiency found in the data.

To model local confusions, it is assumed that there are hue circle regions where the probability of confusion is elevated compared with the incidence of sorting confusions (see, e.g., Fig. 1). Local confusion regions arising from Fig. 1 types of deficiency always present as pairs of regions across the FM100 circle. Let us denote two such confusion regions as I_1 and I_2. Then

$$C_{ij}^{local} = \begin{cases} \exp\left\{-\dfrac{(j-i)^2}{w}\right\}W_i^{-1}, & i,j \in I_1 \text{ or } i,j \in I_2 \\ 1, & i=j \notin I_{1,2} \\ 0, & \text{otherwise} \end{cases}, \tag{2}$$

where w gives the width of the characteristic range of confusion within local confusion regions and W is the normalization factor for the given confusion region: $W_i = \Sigma_{j \in I_{1,2}} \exp\{-(j-i)^2/w\}$, where the summation is over all the caps inside the confusion region of cap i.

3. Global Confusions

Global confusions seen in dichromats are color stimuli confused across the hue circle [[20] pp. 65–69], typically shown as FM100 stimuli pairs connected by a line of confusion [28]. We previously referred to this as an "axis of confusion" [8]. Development of dichromat agent models gave consideration to whether typical FM100 confusion pair axes (e.g., Fig. 2) realistically capture the day-to-day confusions of dichromats, given that some visual processing circumstances help disambiguate global confusion pairs and make global confusions less likely in everyday color judgments. Our models adopt Fig. 2's [28] confusion pairs because (a) occupational evidence suggests that global confusions do arise in everyday practice and (b) FM100 confusion pair axes are consistent with confusions seen in dichromat judged-similarity color-triad performance [15]. Thus, dichromat global confusion pairs exist in practice when similarity is important, as is the case with the FM100 task. Based on Fig. 2, dichromat global confusions are modeled as three pairs of opposing caps from the FM100 hue circle. Let us denote them x_k and $\bar{x}_k$ with $k \in \{1, 2, 3\}$. It is convenient to introduce a function g defined on the set $X_{gl} \equiv \{x_1, \bar{x}_1, \ldots, \bar{x}_3\}$ such that $g(x_k) = \bar{x}_k$ and $g(\bar{x}_k) = x_k$. The global confusion matrix is given by the formula

$$C_{ij}^{global} = \begin{cases} 0.5, & i \in X_{gl} \text{ and } j = i \\ 0.5, & i \in X_{gl} \text{ and } j = g(i) \\ 1, & i = j \notin X_{gl} \\ 0, & \text{otherwise} \end{cases} . \qquad (3)$$

Accordingly, protanope and deuteranope global confusion matrices are separately modeled based on the respective confusion lines shown in Fig. 2.

D. Parameter Estimation Based on Data Analysis

Based on these forms of confusion identified across various types of observers [Eqs. (1)–(3)], simulation parameter settings were derived for different agent types using the relevant human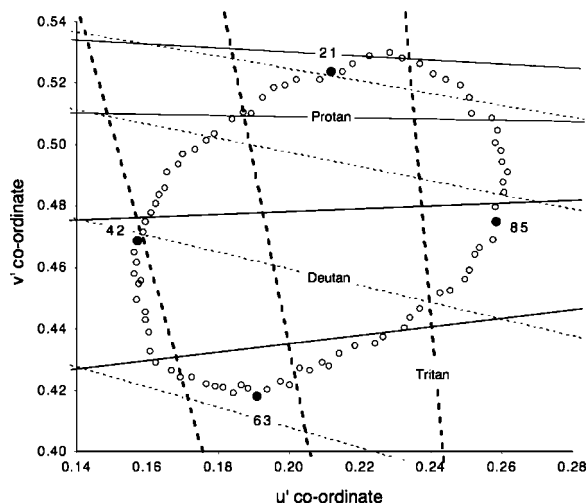 data. Thus, the appropriate FM100 data determine the parameter settings for various forms of "normal trichromat" and "dichromat" agents. Parameter values varying across agent types include p, probability of sorting confusions [Eq. (1)]; I_γ with $\gamma \in \{1, 2\}$, local confusion regions [Eq. (2)]; w, a confusion range value within local confusion regions [Eq. (2)]; and x_k and $\bar{x}_k$ with $k \in \{1, 2, 3\}$, global confusion pairs [Eq. (3)]. Further simulation parameterization details are given in Table 1.

1. Sorting Errors

The probability of sorting errors, p, is calculated as follows. For normal individuals the FM100 data of ten normal trichromat individuals were used to calculate each individual's total number of cap inversions. [29]. The average number of observed inversions across the ten normal individuals equaled 6.8 inversions. Thus, based on these data, on average a normal individual makes 6.8 randomly distributed sorting errors per 85 caps (1.7 inversions per tray). The probability of inversion *per cap* is given by $6.8/85 = 0.08$, that is, 8%. This value was used to model the unbiased sorting error for normal individual performance across the 85 stimuli of the FM 100. Consistent with dichromat characteristic performance, 8% sorting error was also used to model dichromat sorting confusion rates outside local confusion regions and independent of global confusion pairs [30].

2. Local Confusion Regions

For dichromat agents, local confusion regions were based on Fig. 1 results, where protanopes have two confusion regions, $I_1 = [12, 27]$ and $I_2 = [59, 70]$, and deuteranopes regions are $I_1 = [9, 25]$ and caps $I_2 = [51, 63]$, [31]. A dichromat confusion range width parameter w, for estimating cap sequence inversions that occur inside local confusion regions was defined as $w = 10$, also based on Fig. 1 data. Consistent with human observer data, models for normal agents do not include local confusion regions.

3. Global Confusion Pairs

Figure 2 data provide values for dichromat global confusion pairs. Protanope global confusion pairs are caps: $x_1 = 9$ & $\bar{x}_1 = 29$, $x_2 = 1$ & $\bar{x}_2 = 40$, and $x_3 = 74$ & $\bar{x}_3 = 53$. Deuteranopes also have three global confusion pairs: $x_1 = 11$ & $\bar{x}_1 = 21$, $x_2 = 2$ & $\bar{x}_2 = 31$, and $x_3 = 79$ & $\bar{x}_3 = 42$.

4. Summary of the Resulting Agent Models

The following agent confusion definitions were incorporated in our model:

Fig. 2. Dain's depiction of FM100 stimuli in CIE (1976) space [28] (reproduced with permission). Inset lines show three global confusion pairs used for protan (solid lines) and deutan (dotted lines) agents modeled.

Table 1. Simulation Notation

Symbol	Definition	Value
N	Total number of agents	100
n	Total number of hue circle stimuli (FM100 samples)	85
k_{sim}	Parameter defining the pragmatic utility of colors	11
w	*Confusion range* operating in a local confusion region	varies
p	Probability of sorting confusion	varies
C_{ij}	Probability that stimulus i is confused with j	Eqs. (1)–(3)

Normal agents ($C = C^{sorting}$): Probability of confusion with a neighboring cap is $p = 8\%$.

Dichromats ($C = C^{sorting}C^{local}C^{global}$): (*i*) Probability of confusion with a neighboring cap, both inside and outside the confusion region, is $p = 8\%$. (*ii*) Local confusion regions based on Fig. 1 data range from 12 to 27 and from 59 to 70 for protanope agents and 9 to 25 and 51 to 63 for deuteranope agents. Inside the confusion regions, $w = 10$. And (*iii*) Global confusion pairs based on Fig. 2 data: (9,29), (1,40), (74,53) for protanopes, (11,21), (2,31), (79,42) for deuteranopes.

Parameter values that differ from Table 1 are noted in the text. To the degree that the data used in our modeling differ from other observer data in the literature, our observer models would vary accordingly if based on different data. During model development we varied the data underlying the parameterization to evaluate the effect on categorization solutions. Such tests found that altering model features such as the positions of local confusion ranges and global confusion pairs, or varying the values of sorting confusion rates, did not fundamentally alter the main findings presented here or diminish the symmetry-breaking results or category-solution trade-offs reported in Studies 1 and 2 below.

3. POPULATION HUE CATEGORIZATION INVESTIGATIONS

Study 1 and Study 2 consider homogeneous populations to (i) investigate population categorization influences arising from different forms of individual variation within populations and (ii) to provide a foundation for planned comparisons between heterogeneous populations (i.e., in [13]). Population homogeneity is intentionally unrealistic, but is used in the present investigations to isolate the specific influences that arise under the communication dynamics between individuals of particular observer color vision phenotypes.

A. Communication Games Using FM100 Stimuli

Population color naming is achieved by discrimination–similarity communication games involving the 85 FM100 caps. Details of the discrimination–similarity communication game, its variants, its relationship to other population naming evolutionary algorithms, and its rationale as an approach for understanding the evolution of color categorization systems are reported elsewhere [6,8].

Briefly, the goal of the game is for a population of agents to communicate successfully about color stimuli. At the beginning of the game, a large number of potential names, with random meanings, are provided. Agents evolve probabilistic naming strategies for the stimuli using only these names. In a given round of the game, two agents are randomly chosen from the population and two caps are randomly chosen, and named. Each agent's probabilistic naming strategy is updated by its performance in the round. The basic idea of the updating is that if agents successfully communicate about the colors of two caps, or they agree on the caps' names, then the probabilities that they will give the same names to those caps in the future is increased (i.e., the agents are positively reinforced) and appropriate decreasing adjustments are made to the other caps.

To carry out successful communication in a game, it is also required that the two names meet the following coherence requirement. The degree of similarity of two distinct caps is related to the inverse of the smallest number of caps between them. If the degree of similarity of two caps is large (i.e., they are neighboring caps on the circle) and there is not an enormous number of names (as in these simulations), then an evolutionarily effective naming system will assign the two caps the same name. Similarly, names for caps with a small degree of similarity should, in general, be different. The parameter k_{sim} denotes a pragmatic degree of similarity that determines whether two caps should be given the same name or different names. Caps with fewer than k_{sim} caps between them should be given the same name, and those separated by more than k_{sim} caps should be given different names. The value of k_{sim} can be made to vary across the hue circle if some colors have more pragmatic or social utility than others, and it has been shown to influence solutions from idealized populations [8]. Here k_{sim} is held constant to emphasize effects from observer variation.

B. Investigating Homogeneous Population Solutions

Study 1 examines several homogeneous populations (i.e., populations composed of uniformly modeled agents), where each population incorporates a slightly different individual model. Two Study 1 homogeneous populations are reported, namely, populations composed of 100% normal ideal agents and populations composed of 100% probabilistic normal agents. By comparison, Study 2 examines categorization solutions from homogeneous populations of 100% protanopes compared with those of 100% deuteranopes. The results are described below.

1. Study 1: Homogeneous Normal Populations

Populations consisting only of identical normal observers with $p = 0$ (no sorting errors) or realistic normal observers with $p > 0$ (a nontrivial probability of sorting errors) [32] exhibit similar behaviors: starting from any initial condition, after a number of game iterations, both sorts of homogeneous populations converge to optimal, shared, categorization solutions, with all individual agents converging to very similar categorization solutions (i.e., synchronized up to small levels of random noise).

For Table 1 parameter values, such solutions typically consist of four or five distinct color categories of approximately equal size (shown in Fig. 3), as predicted in [6]. Figure 3 shows that for both ideal and probabilistic normal populations, five distinct categories were found. The disagreement for each cap is calculated as a percentage of the population that categorizes the given cap to a category other than the most popular category. We can see that percent disagreement in the ideal population solution [Fig. 3(a), shown scaled by a factor of 10] is comparatively less than the percent disagreement found in the probabilistic normal population solution [Fig. 3(b), un-
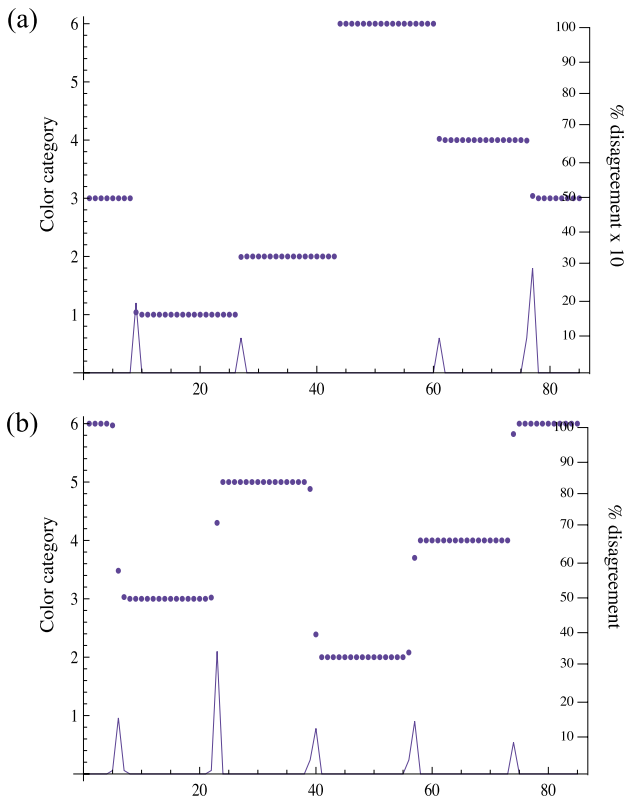
Fig. 3. (Color online) Color categorization and degree of population disagreement in homogeneous normal populations for different values of the sorting error, p. Panels show (a) no sorting errors ($p=0$) and (b) sorting errors with probability $p=0.08$. The horizontal axis is the 85 caps of the FM100. The dotted lines (and the left vertical axis) show population-average categorization solutions for a typical run (after 5×10^7 iterations). The solid lines (and the right vertical axis) show the amount of population disagreement; it is magnified by a factor of 10 in (a). Other parameters are as in Table 1.

scaled]. Figure 3(b) also illustrates the fuzzy category boundaries occurring in the probabilistic normal population solution.

The general finding is that increasing the values of p does not change the general structure of population solutions but increases the amount of uncertainty at category boundaries, making the degree of population agreement on color names near boundaries lower for higher values of p. Aside from this new effect arising from the introduction of parameter p, Study 1's normal population results confirm earlier category solution findings [6].

Solutions observed in Study 1 possess the following characteristic feature: repeated simulations with the same starting parameters produce categorizations with nearly equally spaced boundaries and similar relative category structures, although category position locations can appear shifted by some random rotation from one simulation to another. Put differently, if a given simulation solution partitioned the circular ordering of the FM100 caps into, say, five clear category divisions, then those five categories could be rotated to coincide with the categories of another simulation solution (run with all the same parameters), and the two simulations could be viewed as random rotations of each other. Thus, various forms of so-

lutions are all equally optimal solutions. The fact that solutions are equivalent (or self-similar) with respect to rotations around the circle is a formal *symmetry* property of these solutions that has been observed here across multiple population simulations. This finding was predicted by earlier analytical results [6] and should be noted, because equally interesting observations of *symmetry breaking* are presented below.

2. Study 2: Homogeneous Dichromat Populations
Simulations were run on agent populations composed entirely of 100% protanopes and 100% deuteranopes. Despite the fact that the observer model underlying these agents is very different from the normal model of Study 1, each category solution from homogeneous dichromat populations exhibited an overall category structure similar to that of normal populations. The difference can be seen by running many evolutionary simulations starting with the same parameter values. Figures 4 (for protanopes) and 5 (for deuteranopes) present boundary location frequencies observed across many such solutions. Both figures' histograms show distributions of solutions that are strikingly nonuniform. Consider the leftmost bottom histogram in Fig. 4, which shows boundary location frequencies for all solutions from 1,000 random protanope simulations. The boundaries occur most frequently at caps 8, 29, 52, and 74. A clear picture also emerges by examining only four-category solutions shown in the bottom-middle histogram in Fig. 4. Boundary locations distributed across these solutions are almost identical to each other, mostly occurring at caps 8, 30, 52, and 74. As predicted and similar to that observed elsewhere for idealized models of dichromats [8], the nontrivial psychophysical transformation characterizing realistic dichromat data leads to a symmetry breaking.

By comparison, Study 1's similar boundary frequency histograms from homogeneous normal population simula-
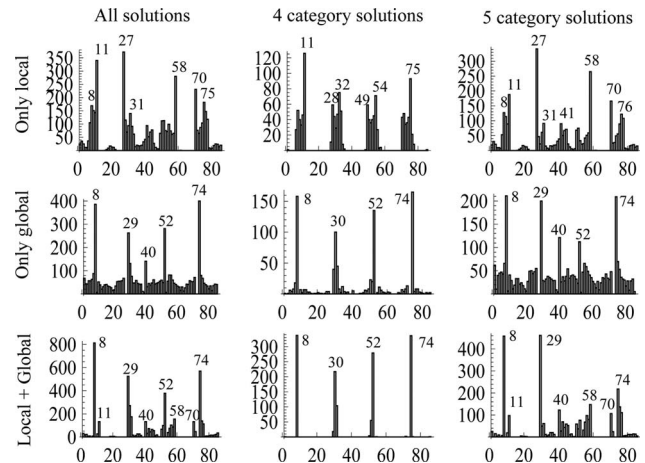

Fig. 4. Boundary location histograms from 1,000 simulation solutions by homogeneous protanope populations. Horizontal axes show the FM100 85 caps. Vertical axis shows frequency with which a color boundary was established at a given FM100 cap. Results are shown separately for all observed solutions (histograms at left), four-category solutions (middle), and five-category solutions (right). Top row, results under local confusion regions; middle row, results under global confusion pairs; bottom row, results for both confusion features. Other parameters are in Table 1 and as described in Section 2.
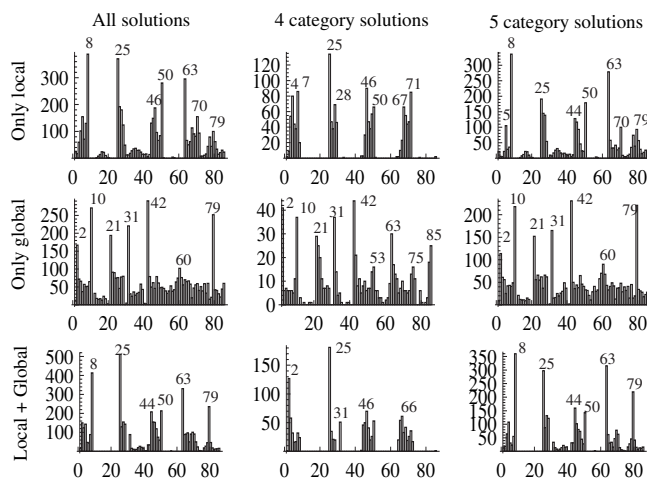
Fig. 5. Boundary location histograms from 1,000 simulation solutions by homogeneous deuteranope populations. Figure layout and parameters are as in Fig. 4.

tions (not shown) appear as essentially uniform, unbiased distributions without any clear maxima, except for slight randomness caused by the finiteness of our simulations. Irregularity of boundary locations across many solutions suggests that optimal category boundaries are not tied to specific stimulus locations for homogeneous normal populations. In contrast, dichromat populations optimally have color boundaries with preferred locations.

While homogeneous populations of dichromats are not found in the real world, the present simulations involving homogeneous populations of dichromat agents are very informative from a theoretical standpoint. In particular, they help explain what features in the observer model are responsible for symmetry breaking and how exactly local and global confusions influence population color boundary locations.

Local confusions. The top rows of Figs. 4 and 5 show simulation results using dichromat agent models that include local confusion constraints only (no global confusion pairs were included in the simulations). For these results protanope (Fig. 4) and deuteranope (Fig. 5) boundaries are frequently located in well-defined segments along the hue continuum, with few or no boundaries found between caps 11 and 27, or between caps 58 and 70 for protanopes. Similar results are depicted in the top rows of Figs. 6 and 7, where local confusion regions are marked by thick black circular arcs and dashed double arrows define observed color boundary locations (the results depicted in Figs. 6 and 7 correspond to those in Figs. 4 and 5 results, respectively).

A general finding is that no boundaries occur inside any local confusion regions. For five-category solutions (top-right graphics) the two most frequent solutions are drawn as inscribed pentagons. Overall, results suggest that the local confusion regions modeled from the data of Fig. 1 tend to repel color boundaries.

Global confusion pairs. The influence of global confusion pairs on categorization solutions is shown in the middle rows of Figs. 4 and 5, where color boundaries are biased to a small subset of stimuli. For example, protanope four-category solutions almost always have boundaries at caps 8, 30, 52, 74 (Fig. 6, left column, middle row),

indicating that the boundaries of the most frequent four-category solution align with four out of the six global confusion pair caps (i.e., pairs marked by arrows connected across the circle). Five-category solutions are more complicated because it is hard to find one nearly regular pentagon with vertices at global confusion stimuli (Fig. 6, middle row on left). In this case, the populations established several solutions in which three out of five boundaries aligned with global confusion stimuli. Similar findings are seen for deuteranopes, which produce three most common four-category and five-category configurations (Fig. 7).

These results (along with those from earlier research [6,8]) show that global confusion pairs affect categorization by attracting boundaries through symmetry breaking and providing necessary perceptual anchors (for some observers) in the categorization system of a population [33].

Technically speaking, the notion of color boundaries is ill-defined in dichromat populations with global confusion pairs. This is because in such populations, optimal categorization solutions are not exactly the same as in populations of normals. That is, even though they do consist of disjoint regions belonging to one category, there are also "defects" near the location of global confusion pairs. At these locations, two types of solutions are observed: (i) one cap is classified as having a different color category from its neighbors, such as AAAABAAAA (here, cap number 5 has category B and all its neighbors have category A) and (ii) one cap at the boundary between two categories is classified as a third category, such as AAAABCCCC (here, one cap at the boundary between categories A and C is classified as B).

In Figs. 4 and 5, such defects (at most, six per solution) were smoothed out: that is, B replaced A in type (i) defects, and by either A or C in type (ii) defects. The existence of these defects can be understood as follows: in the presence of global confusions the color space of dichromats has effectively a noncircular geometry, similar to that shown in our previous studies [8], where parts of the circle were collapsed onto each other. Note that many forms of this collapse were investigated: a single point of collapse across the hue circle, a full line, or any intermediate collapse. All of these served to break symmetry in the population solutions observed [8]. In the presence of global confusion pairs, then, the geometry of the optimal solution changes accordingly.

Local and global confusion trade-offs and parameter variation. Given the above observations, the combination of these constraints clearly produces strong anchoring tendencies for color boundaries at a subset of locations along the circle, generally resulting in boundaries being attracted by global confusion pairs and repelled by local confusion regions. This is illustrated in Fig. 7, left column. For example, when global confusion features are used as constraints in the simulations (middle row), the three preferred four-category solutions are optimized to (i) approximately equi-partition the circle and (ii) have two boundaries near global confusion points. However, when both local and global confusion features are used (bottom row), the constraints on solutions become more stringent because local confusion features specifically restrict color boundaries from forming inside a local confu-

sion region (e.g., see top row, Fig. 7). Thus, whereas three four-category solutions arise for simulations using only global confusion features, only two four-category solutions arise when both local and global features are used in the simulations.

Depending on the dichromat type and the number of categories, local and global confusion features can alternate as the more restrictive influence on color category boundary formation. For example, for protanope four-category solutions, global confusions exert a greater influence on boundary location (Fig. 4, middle column). By comparision, for deuteranopes local confusions exert a greater influence on their four-category solutions' boundary locations (Fig. 5, middle column).

The protanope and deuteranope agents in these studies are characterized by parameter values estimated from individual human data. However, the sample size of data is small, which makes the error in parameter estimation high. Therefore it is important to investigate how particular parameter choices affect the results. Experiments were conducted using various positions of local confusion regions with respect to global confusion pairs, and while resulting boundary locations may change, the general conclusions reported here remain robust.
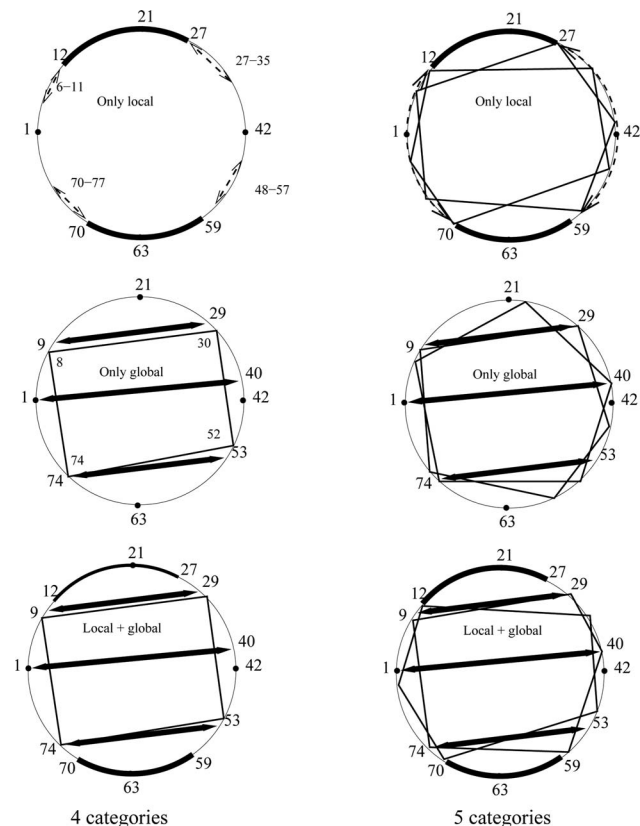

Fig. 6. Confusion parameter settings shown with results from homogeneous protanope solutions (from Fig. 4). Top row, local confusions; middle row, global confusions; bottom row, both confusions. The circle depicts the FM100 caps. Caps 1, 21, 42, and 63 provide arbitrary points of reference. Thick black arcs with end caps show local confusion regions. Two-point thick black arrows with confusion pair caps show global confusions. Typical four-category (left), and five-category solutions (right) are shown. In the case of local confusions (top row), dashed double-arrowhead lines mark regions where boundaries occur.
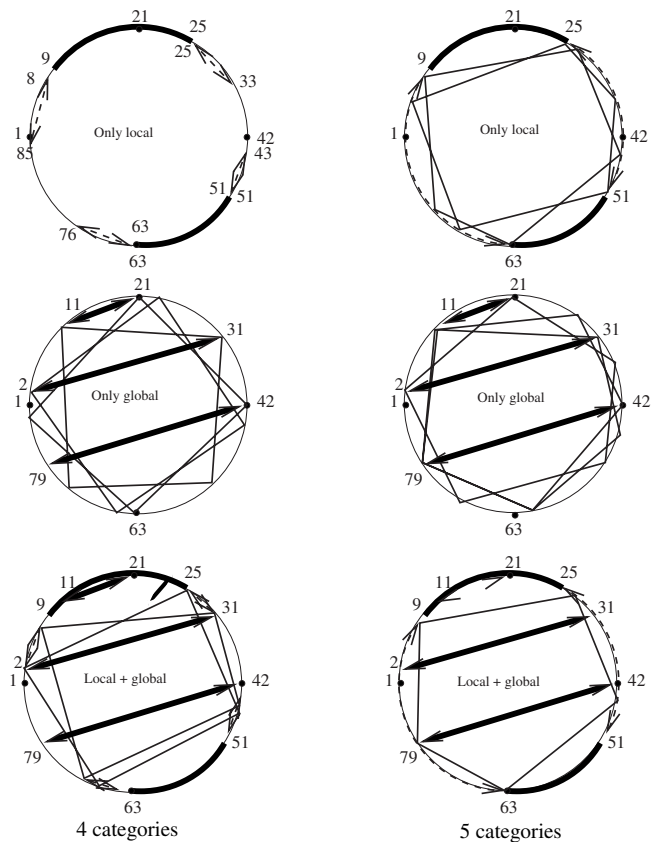

Fig. 7. Confusion parameter settings shown with results from homogeneous deuteranope solutions (from Fig. 5). Figure layout and features are as in Fig. 6. Unlike the protanope model (Fig. 6), the deuteranope model has a local confusion region that coincides with a global confusion pair (bottom row) and has local confusion regions larger than those in the protanope data. Both differences affect category boundary robustness.

Also, studies performed with different values of w (the confusion width) and p, (the probability of sorting errors) show that the value of p has a minimal effect on solutions. However, decreasing the value of w to low values (say, $w = 1$) alters solutions slightly. In particular, large values of w make local confusion regions virtually impenetrable to boundaries, whereas when $w = 1$ there are some solutions whose boundaries are located inside the local confusion region. Those solutions are still quite infrequent, and they disappear as w is increased to more realistic values.

4. DISCUSSION

Studies 1 and 2 provide (i) categorization solutions under different homogeneous perceptual biases, and (ii) a means for investigating mechanisms underlying previously observed symmetry breaking effects [8], in populations composed entirely of realistic dichromat agent models.

Study 1 examined populations consisting of identical normal observers with $p = 0$ (no sorting errors) and several variations of $p > 0$ (nontrivial probability of sorting errors). Across several investigations p was varied, and the general consequence of increasing probabilistic sorting errors in the agent models was decreases in population solution agreement *at color category boundaries*. Aside from

this, increases of probabilistic sorting errors produced no other effects on category solutions. This result is interesting from the perspective of human color categorization theory, because it suggests that varying precision in individual category assignments during communication does not hinder the formation of a shared population color categorization system. Rather, varying of precision simply adds to the degree of classification uncertainty—or fuzziness—observed at population color category boundaries. Study 1's findings for sorting error increases resemble the null effects seen following random observer variation in other color category simulation research (see [3], p. 517).

Study 2 investigated realistic approximations of dichromat individual color perception variation to understand the effect of different observer features on population color category evolution. Dichromat population simulations show that trade-offs were common among the features of various agent models. These features balanced in a dynamic fashion during the formation and stabilization of near-optimal color categorization solutions.

All the observed solutions of both Study 1 and Study 2 reached stabilization by maximizing successful color communications among agents. This was achieved in ways compatible with an optimal partitioning theory of color space that uses an Interpoint Distance heuristic [9,34,35]. By varying the discrimination features modeled, insights were gained concerning the mechanisms involved in the formation of category boundaries. These findings provide likely insights for human color categorization evolution.

Together, Studies 1 and 2 support the suggestion that varying individual perceptual features influences population color categorization solutions. Results show that homogeneous populations of simulated normal observers produce category solutions that differ in important ways from those produced by homogeneous populations of realistic dichromat agents. In addition, local and global confusion analyses suggest a possible universal mechanism for the stabilization of population color categorization systems. Similar color-naming solution dynamics were seen across populations even when the underlying population response models had different perceptual biases. Finally, here we examined situations involving agents made to resemble a variety of real observers with fixed k_{sim}, whereas previous investigations examined populations with ideal heterogeneous color observers with fixed and variable k_{sim} [8]. Despite these differences, a general result of the present simulations and others [6,8], is that the discrimination–similarity game evolves population naming behavior that is near theoretically optimal. See [6] for details about optimal naming behavior.

5. SUMMARY OF FINDINGS

Our findings can be summarized as follows:

1. In homogeneous populations of realistic dichromat observers, local and global confusions exert significant symmetry-breaking effects on categorization solutions. This contrasts with unsystematic error variations or random sorting confusion variations, which have little impact on category solution stabilization.

2. Varying levels of normal-observer sorting confusions primarily decreases population agreement at color category boundaries.

3. Dichromat global confusion pairs break symmetry in categorization solutions by anchoring category boundaries.

4. Dichromat local confusion regions break symmetry in categorization solutions by repelling category boundaries.

5. Realistic approximations of observer types confirm earlier symmetry breaking and confusion axis findings from idealized populations [8]. Such modeling of color categorization dynamics based on realistic data has not, to our knowledge, been previously attempted. The present findings underscore the importance of tracking population heterogeneity when modeling shared color category systems or when empirically studying human color categorization (see discussion in [36]).

6. Category solutions are shaped by the observer features employed, but solutions obtained under such constraints are easily modified by introducing external factors, such as variable color utility (see [8]).

By design, our previous investigations constrained both the realism of the individual observer models and the population models used [6,8]. By comparison, here individual observer models were realistic while the populations considered were unrealistically uniform. Despite the latter intended limitation, some universal tendencies can be suggested by the result for the present population color categorization system evolution:

(i) Minimal impact of unsystematic perceptual variation (e.g., random sorting error) on categorization solutions.

(ii) Substantial constraints imposed on solutions by systematic perceptual variation.

(iii) Countervailing mechanisms (arising from perceptual variation) that trade off in the process of arriving at stable categorization solutions.

(iv) Increases in trade-off demands as perceptual constraints (e.g., color confusion pairs and regions) become more varied or more frequent in a population or engage larger areas of color space.

It seems likely that some of the categorization solution tendencies observed here suggest mechanisms that may similarly underlie universal tendencies in color categorization systems of human populations. In a companion paper ([13], this issue) we pursue further testing of these issues using approximations of both realistic individual and realistic population models.

REFERENCES AND NOTES

1. P. Kay and T. Regier, "Resolving the question of color naming universals," Proc. Natl. Acad. Sci. U.S.A. **100**, 9085–9089 (2003).

2. T. Belpaeme and J. Bleys, "Explaining universal color categories through a constrained acquisition process," Adapt. Behav. **13**, 293–310 (2005).

3. L. Steels and T. Belpaeme, "Coordinating perceptually grounded categories: a case study for colour," Behav. Brain Sci. **28**, 469–529 (2005).

4. L. D. Griffin, "The basic colour categories are optimal for classification," J. R. Soc., Interface **3**, 71–85 (2006).

5. M. Dowman, "Explaining color term typology with an evolutionary model," Cogn. Sci. **31**, 99–132 (2007).

6. N. L. Komarova, K. A. Jameson, and L. Narens, "Evolutionary models of color categorization based on discrimination," J. Math. Psychol. **51**, 359–382 (2007).

7. A. Puglisi, A. Baronchelli, and V. Loreto, "Cultural route to the emergence of linguistic categories," Proc. Natl. Acad. Sci. U.S.A. **105**, 7936–7940 (2008).

8. N. L. Komarova and K. A. Jameson, "Population heterogeneity and color stimulus heterogeneity in agent-based color categorization," J. Theor. Biol. **253**, 680–700 (2008).

9. T. Regier, P. Kay, and N. Khetarpal, "Color naming reflects optimal partitions of color space," Proc. Natl. Acad. Sci. U.S.A. **104**, 1436–1441 (2007).

10. M. A. Webster, S. M. Webster, S. Bharadwadj, R. Verma, J. Jaikumar, J. Madan, and E. Vaithilingam, "Variations in normal color vision. III. Unique hues in Indian and United States observers," J. Opt. Soc. Am. A **19**, 1951–1962 (2002).

11. M. A. Webster and P. Kay, "Individual and population differences in focal colors," in *Anthropology of Color: Interdisciplinary Multilevel Modeling*, R. E. MacLaury, G. V. Paramei, and D. Dedrick eds. (Benjamins, 2007), pp. 29–53.

12. Delwin T. Lindsey and Angela M. Brown, "Universality of color names," Proc. Natl. Acad. Sci. U.S.A. **103**, 16608–16613 (2006).

13. K. A. Jameson and N. L. Komarova, "Evolutionary models of categorization. II. Investigations based on realistic observer models and population heterogeneity," J. Opt. Soc. Am. A **26**, 1424–1436 (2009).

14. T. N. Cornsweet, *Visual Perception* (Academic, 1970).

15. R. N. Shepard and L. A. Cooper, "Representation of colors in the blind, color blind, and normally sighted," Psychol. Sci. **3**, 97–104 (1992).

16. D. Farnsworth, *The Farnsworth–Munsell 100 Hue Test for the Examination of Color Vision* (Munsell Color Company, 1949/1957).

17. K. Mantere, J. Parkkinen, M. Mäntyjärvi, and T. Jaaskelainen, "Eigenvector interpretation of the Farnsworth–Munsell 100-hue test," J. Opt. Soc. Am. A **12**, 2237–2243 (1995).

18. R. S. Cook, P. Kay, and T. Regier, "The World Color Survey database: history and use," in *Handbook of Categorisation in Cognitive Science*, H. Cohen and C. Lefebvre, eds. (Elsevier, 2005), pp. 223–242.

19. T. Regier, P. Kay, and R. S. Cook, "Focal colors are universal after all," Proc. Natl. Acad. Sci. U.S.A. **102**, 8386–8391 (2005).

20. J. Birch, *Diagnosis of Defective Colour Vision*, 2nd ed. (Butterworth-Heinemann, 2001).

21. J. H. Nelson, "Anomalous trichromatism and its relation to normal trichromatism," Proc. Phys. Soc. **50**, 661–702 (1938).

22. J. Pokorny, V. C. Smith, G. Verriest, and A. J. L. G. Pinckers, *Congenital and Acquired Color Vision Defects* (Grune & Stratton, 1979).

23. G. Wyszecki and W. Stiles, *Color Science: Concepts and Methods, Quantitative Data and Formulae*, 2nd ed. (Wiley, 1982).

24. L. T. Sharpe, A. Stockman, H. Jägle, and J. Nathans, "Opsin genes, cone photopigments, color vision, and color blindness," in *Color Vision: From Genes to Perception*, K. R. Gegenfurtner and L. T. Sharpe, eds. (Cambridge U. Press, 1999), pp. 3–51.

25. B. Sayim, K. A. Jameson, N. Alvarado, and M. K. Szeszel, "Semantic and perceptual representations of color: evidence of a shared color-naming function," J. Cogn. Culture **5**, 427–486 (2005).

26. Farnsworth–Munsell Scaling Software, Version 2.1 (MacBeth Division of Kolmorgen Corporation, 1997).

27. D. Farnsworth, "The Farnsworth–Munsell 100-Hue and Dichotomous Tests for color vision," J. Opt. Soc. Am. **33**, 568–578 (1943).

28. S. J. Dain, "Clinical colour vision tests," Clin. Exp. Optom. **87**, 276–293 (2004).

29. The number of sequence inversions (of adjacent caps) needed to recreate a perfect order from the sorting data.

30. Assuming that dichromats perform similarly to normals away from confusion axes, despite the suggestion of error-free performance outside dichromat local confusion regions in Fig. 1.

31. These confusion regions closely resemble some [17] based on the standard Farnsworth method of scoring [16].

32. $P=0$ models an *ideal* normal-observer's sorting of the FM100 85 caps with zero error (see [7]), whereas a realistic normal-observer model sorts the 85 caps with probabilistic ($p>0$) error.

33. W. R. Garner, *The Processing of Information and Structure* (Erlbaum, 1974).

34. K. Jameson and R. G. D'Andrade, "It's not really red, green, yellow, blue: An inquiry into cognitive color space," in *Color Categories in Thought and Language*, C. L. Hardin and L. Maffi, eds. (Cambridge U. Press, 1997), pp. 295–319.

35. K. A. Jameson, "Culture and cognition: What is universal about the representation of color experience?" J. Cogn. Culture **5**, 293–347 (2005).

36. K. A. Jameson, "Sharing perceptually grounded categories in uniform and nonuniform populations," Behav. Brain Sci. **28**, 501–502 (2005).